SSRG International Journal of Electrical and Electronics Engineering
ISSN: 2348-8379/ https://doi.org/10.14445/23488379/IJEEE-V11I6P119

Volume 11 Issue 6, 167-181, June 2024

Original Article

Efficient Weather-Adaptive Smart Lighting System: Analysis of LED Performance at Different Operating Conditions and Sensor Input Signals

Tanumay Halder[1], Biswanath Roy[2]

[1]*Electrical Engineering Department, Cooch Behar Government Engineering College, West Bengal, India.*
[2]*Electrical Engineering Department, Jadavpur University, West Bengal, India.*

[1]*Corresponding Author : tanumay.halder6@gmail.com*

Received: 09 April 2024 Revised: 11 May 2024 Accepted: 09 June 2024 Published: 29 June 2024

Abstract - *Improving visibility on streets is crucial for maintaining traffic speed, reducing accidents, and boosting confidence in adverse weather like fog and rain. This research introduces a unique approach to enhance visibility during such conditions by adjusting the CCT of LED lights from 6500K to 2700K. The system collects data from weather APIs and rain sensors to change the color of RGB LEDs on the street surface, while PIR sensors adjust the brightness based on detected objects. During fog and rain, the system shifts to 2700K CCT, reverting to 6500K in normal weather. Graphical plots depict the current, voltage, and power data of the LEDs alongside sensor signal capturing. A prototype confirms the proper functionality of the control logic. Electrical parameters of LED consumption show no change despite color adjustment, highlighting energy efficiency as brightness decreases in the absence of objects. Results demonstrate the responsive nature of the prototype, significantly boosting user confidence on streets in adverse weather.*

Keywords - *Streetlighting, Rain, Fog, XBee, Visibility.*

1. Introduction

For the development of smart cities, the adoption of intelligent street lighting is a major factor in saving energy, reducing costs, increasing traffic speed, and decreasing traffic accidents. While illuminating a street area, the priority is to save energy and reduce costs. So, it is essential to be cautious when designing lighting systems to ensure that the quality of light is not compromised. Different articles on outdoor lighting [1, 2, 6, 12,14,16,19, 21-27], color formation by RGB LED [8, 13], and fog-related research [10, 11] have been studied to perform this research work. In streetlighting, identification of any object and its direction of movement is very crucial for any street surface user whether it is a motor driver, cyclist, or pedestrian. If street surface users do not make proper identification of objects, it results in lethal collision, injuries, and property damage.

From one of the experimental studies, it is found that adequate street lighting can reduce 65% of fatal accidents, 30% of injuries, and 15% in reduction in property damage at nighttime [3]. Another study suggests that adaptation of the modernization of streetlights can reduce 36% of nighttime crashes [4]. According to another study, nighttime crashes can be reduced by the modernization of streetlights and increasing street surface horizontal foot-candelas values [5]. In another study, the authors suggest that fog is the main cause of traffic accidents due to reduced visibility and increased anxiety, resulting in decreased driving ability and concentration [6]. In another study, the author suggests horizontal illuminance is necessary to provide a suitable visual environment for pedestrians [18]. After reviewing the papers', it is very clear that there is a correlation between street surface accidents and street lighting. It is very important to ensure adequate visibility under varying weather conditions for safety and security and to identify moving objects properly on the surface. It is observed during foggy and rainy weather conditions that the visibility of users has been reduced. As a result, the speed of traffic becomes less, and different types of fatal accidents happen.

In another study, the authors concluded that a light source with low color temperature (CCT) would be recommended for any areas with frequent fog formation. Lighting systems with variable CCT configurations should be considered to produce lower CCT in low-visibility weather conditions [7]. In another existing literature, authors experimentally tested that the fog formation amount is increased when the amount of humidity in the air is higher, and air vaporizers can directly affect the humidity levels in the surrounding air by adding moisture through vaporization [9]. Based on the literature

review, it is evident that to reduce street accidents and improve visibility in adverse weather conditions, weather responsive lighting system is necessary.

This system should be capable of enhancing visibility on street surfaces by detecting adverse weather conditions and automatically adjusting LED lights from higher CCT values to lower CCT values. In another existing literature, the authors developed such a lighting scheme where in every street lighting pole, two different lighting fixtures are installed, and depending on the weather situation, the microcontroller actuates one of the two lighting fixtures (Change CCT between 3000K and 5000K) suitable for the specific weather condition. In that literature, a relay is considered, which tunes a specific LED light between two LED lights at every street light pole. However, in that scheme, the authors have not provided any solution where only one light source is capable of providing a dynamic CCT-based color variation scheme [21].

From the existing literature review, it is observed that changes in Correlated Color Temperature (CCT) over street surfaces are important during varying weather conditions like rain and fog, as these conditions adversely affect the visibility for street surface users. The literature review also indicates that the authors have proposed two lighting fixtures on each pole. However, a research gap exists in the literature concerning the use of a single lighting fixture to reduce both installation and running costs. Addressing this gap, this work proposes a lighting system that utilizes a single lighting fixture on each street lighting pole, thereby reducing both installation and running costs. To enhance visibility, it is necessary to change the CCT of LED street lights to increase visibility for lighting requirements. In this work, a hardware setup is developed that assists in controlling the brightness of LED light and it's CCT. During foggy weather, visibility is observed to be reduced beyond normal conditions. This research aims to fulfil these requirements.

2. Features of the Designed Lighting System

- The designed system collects fog data from a third-party API and transmits information to the main microcontroller, enabling it to recognize foggy weather conditions and adjust the RGB LED color accordingly.
- The smart lighting system itself adjusts the street light color without the need for extra components or reliance on another light source to switch between cool white and warm white.

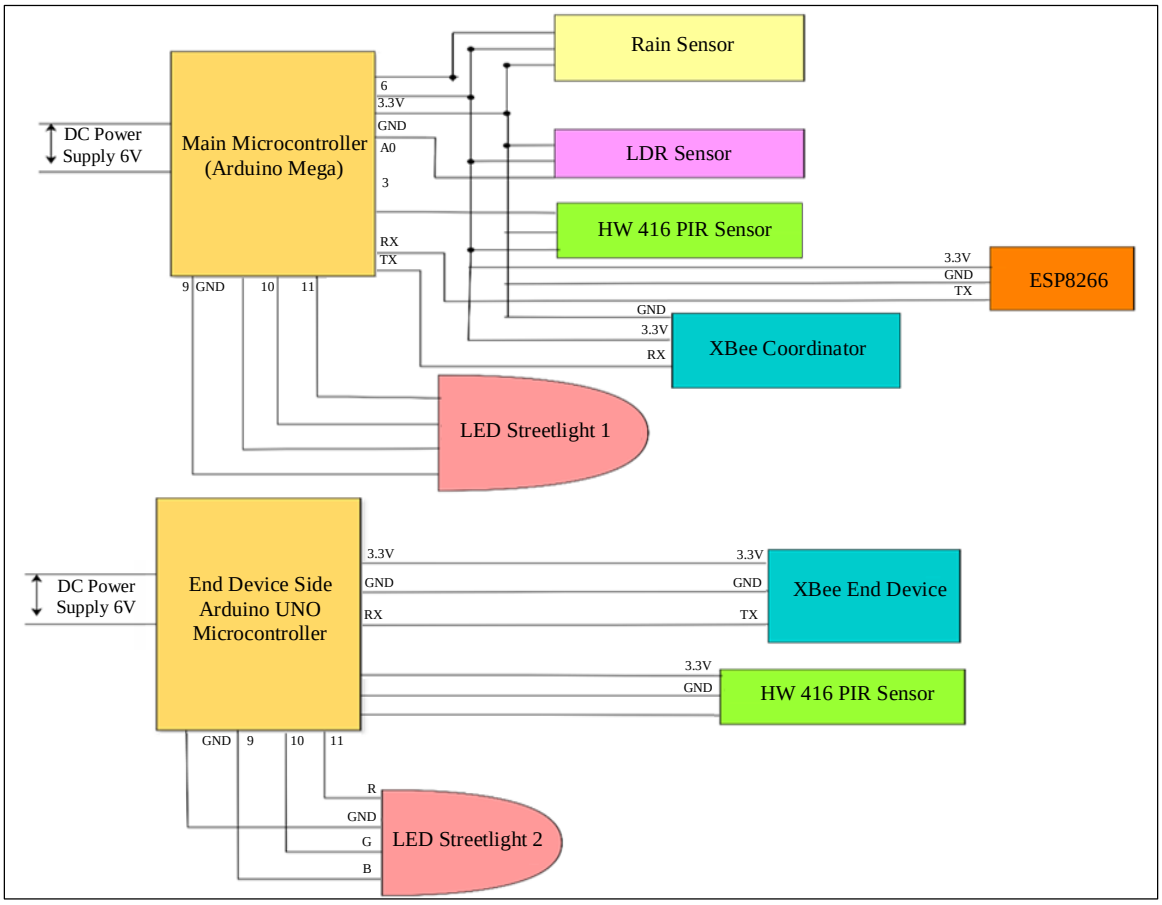

Fig. 1 Block diagram of designed lighting system

- The designed system conserves energy by dimming the LED street light to 25% of full brightness when there is no object present over the street surface.
- While some research proposes increasing LED brightness during rainy weather, this system differs by adjusting the CCT from cool white to warm white to enhance visibility without increasing electricity consumption. This is one novelty of the work. In the existing literature, authors have increased the brightness of the lighting system with an increase in electrical energy [27].
- Another novelty of the designed system is its capacity to adapt to both foggy and rainy weather conditions simultaneously without an increase in electrical energy consumption. This integration is achieved through a single street lighting system that adjusts LED brightness and color settings, effectively improving visibility for street surface users.

3. Designed Lighting System-Conceptual Block Diagram

In this developed weather-adaptive hardware system, the Arduino Mega [21, 22,] serves as the primary microcontroller, while the Arduino Uno functions as the microcontroller on the end device side. The Arduino Mega is connected to an LDR sensor, HW 416 PIR sensor, DHT11 sensor [12], and rain sensor. To develop a weather-adaptive hardware system, the Arduino Mega serves as the primary microcontroller, while the Arduino Uno functions as the microcontroller on the end device side.

ESP8266 is an open-source microcontroller unit and a combination of both software and hardware development modules. The ESP8266 Wi-Fi module has 30 pins and operates at 3.3V. This module is utilized to retrieve fog data of the area from the weather API and subsequently transmit the information to the main microcontroller for adjusting the RGB LED connected to it.

XBee wireless connection module is utilized to transmit data signal generated by the Arduino Mega over other street lighting end device side, XBee is connected to Arduino Uno, which is linked to the LED streetlight. The Arduino Mega is based on the ATmega2560 microcontroller, featuring 54 digital input and output pins, including 15 PWM pins, 16 analog pins, 4 UART ports, and a 16MHz crystal oscillator.

The Arduino Uno, powered by an 8 bit Atmega328P microcontroller, comprises 6 analog pins and 14 digital input/output pins, with 6 of them usable as PWM pins. The XBee s2c module, a variant of the RF module, facilitates multiple communication protocols and interfaces with almost any type of microcontroller.

XBee s2c module operates at ZigBe mesh communication protocol. It provides wireless communication to end-point devices. The connectivity range of the XBee S2C module [15] is approximately 400 feet indoors and 4000 feet outdoors. This communication range can be extended by adding more XBee modules [22, 15] to the network. In this developed system, XBee is configured in AT mode [15] for sending and receiving control signals. Streetlights are connected to the microcontroller, and the microcontroller is connected to its XBee module via the Tx/Rx pins. The XBee-based streetlight network is secured, as it establishes a communication network whenever any device shares the same channel and PAN ID. The conceptual block diagram of the designed lighting system is shown in Figure 1.

This street light prototype is equipped with the XBee wireless module to communicate with other street lights as well as with the ESP8266 module to extract fog data from weather API. XBee module uses UART protocol to communicate with the microcontroller. This system is also equipped with sensors like a rain sensor, LDR sensor, and PIR sensor module.

4. Designed Lighting System- Functional Description

In the control scheme shown in Figure 2, initially, the microcontroller reads data from the LDR sensor to determine the availability of daylight. If it senses daylight is present, then sent a signal to switch off streetlights, which are connected to the same XBee network. If daylight is not present then it sends instructions to switch on RGB LED [8, 13] lights at CCT of 6500K and proceed to read data from the ESP8266 WIFI module. If the microcontroller senses weather is foggy then tunes RGB LED at CCT of 2700K.

Then, proceed to read data from the PIR sensor for sensing object movement data. When no object is in motion, the brightness of the RGB LED is reduced to 25% of its full capacity; otherwise, it remains illuminated at 100% brightness. In Figure 5, as a cyclist has just passed through a streetlight pole in both subfigures (i) and (ii), the LED light is dimmed to 25% of its full brightness behind the cyclist, while the two LEDs on the front side adjust their brightness to 100%. When no object is in motion, the brightness of the RGB LED is reduced to 25% of its full capacity.

On the other hand, as the PIR sensor detects the presence of an object, it sends a signal to the microcontroller to increase the brightness of the LED streetlight to 100%. If the microcontroller senses its normal weather, then proceed to read data from the rain sensor. If rain is detected, the LED streetlights will adjust to a color temperature of 2700K.

Simulating warm white light, suitable for foggy weather conditions. The LED occurring then tunes LED streetlights at CCT of 2700K or at a warm white color, which is considered a foggy weather condition. Otherwise, it continues to emit at a

CCT of 6500 K, which signifies a clear visible condition. The conceptual detail functioning of all components is shown in Figure 3. In every step of tuning LED streetlights, the same signal is transmitted via the XBee coordinator to the XBee End Devices [15] for reproducing identical lighting environments over the other streetlights connected in the same network. In Figure 4, a workflow process indicates the functional diagram at the XBee end device side. Where the XBee end device receives the signal sent by the XBee coordinator and sends it to the XBee end device side microcontroller. XBee end device side microcontroller scans whether the XBee coordinator sends any data signal or not. If it senses such a signal, it instantly detects and stores it in its memory. It then reads the stored data signal and switches on the LED streetlight according to the received signal. Instantly, it sends a delivery message to the XBee coordinator to inform it of the received message. Building a secure XBee network between the XBee coordinator and the XBee end device system verifies the same channel and PAN ID [15]. This verification makes the XBee network more secure than any other network. XBee can operate both in AT and API modes. In this scheme, AT mode is selected, and the main microcontroller sends data packet control signals to other microcontrollers via the XBee network for switching streetlights as per situation demands.

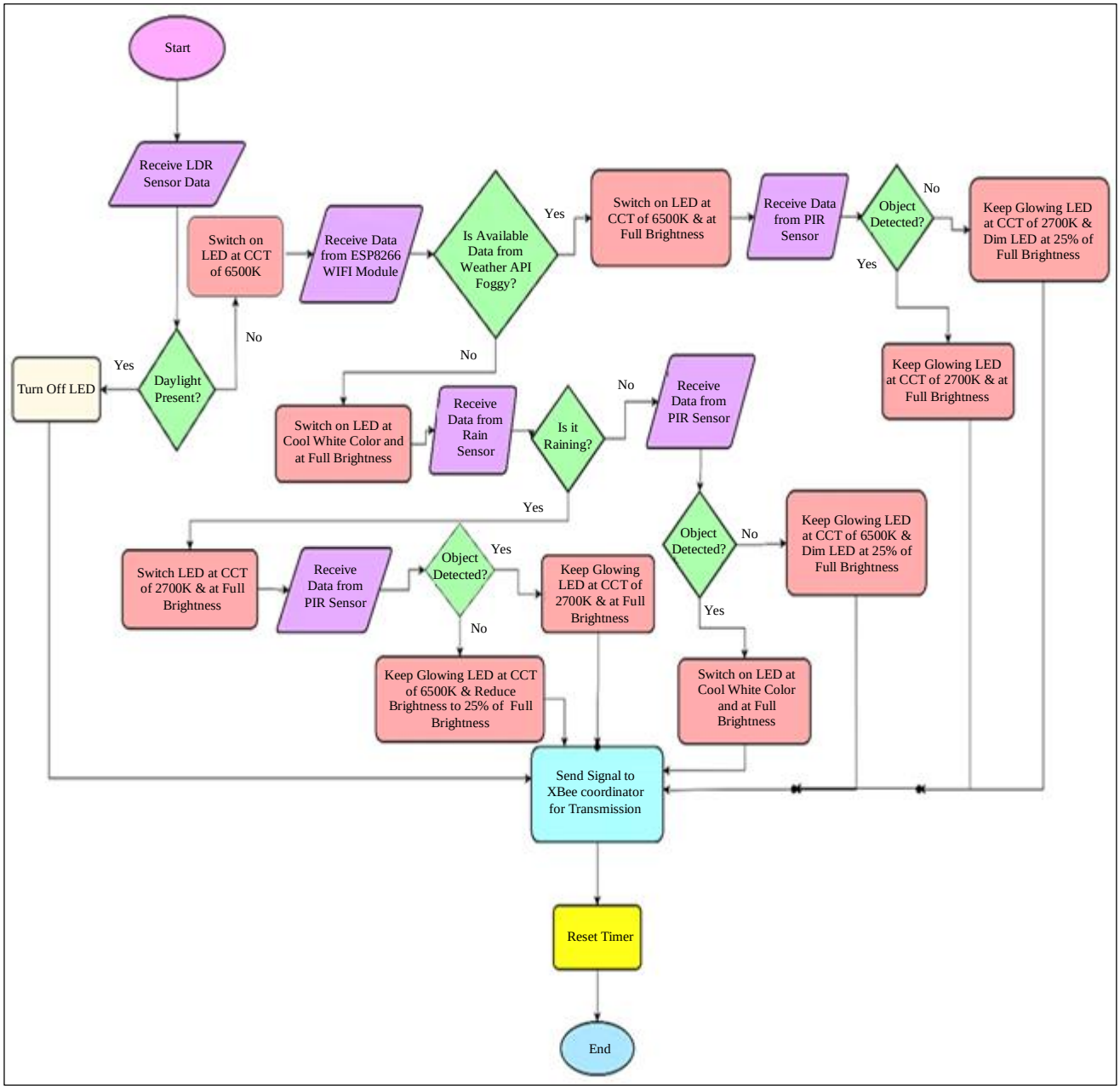

Fig. 2 Flowchart of main microcontroller side operation

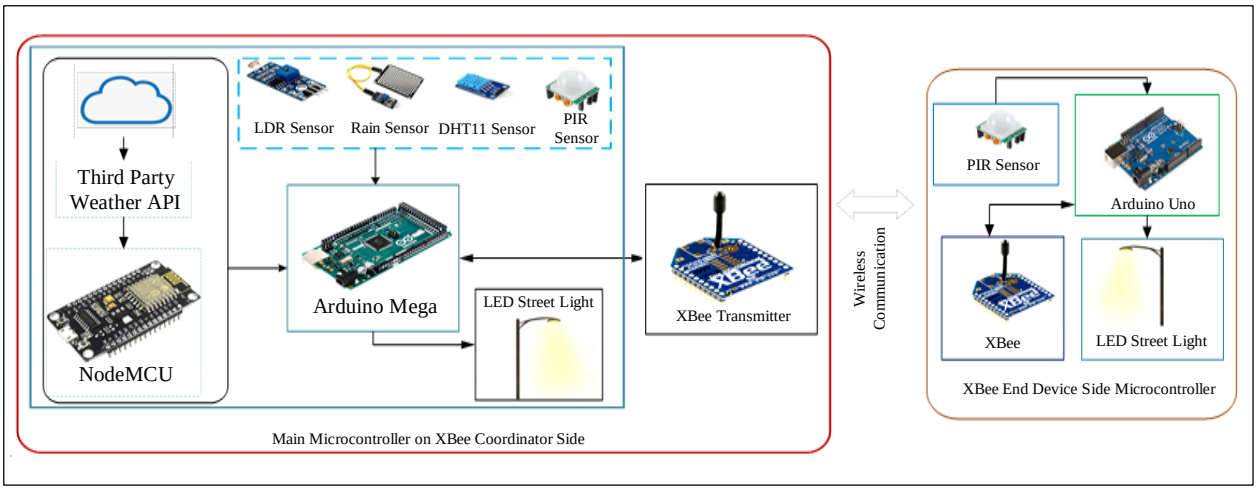

Fig. 3 Conceptual functional diagram of designed system

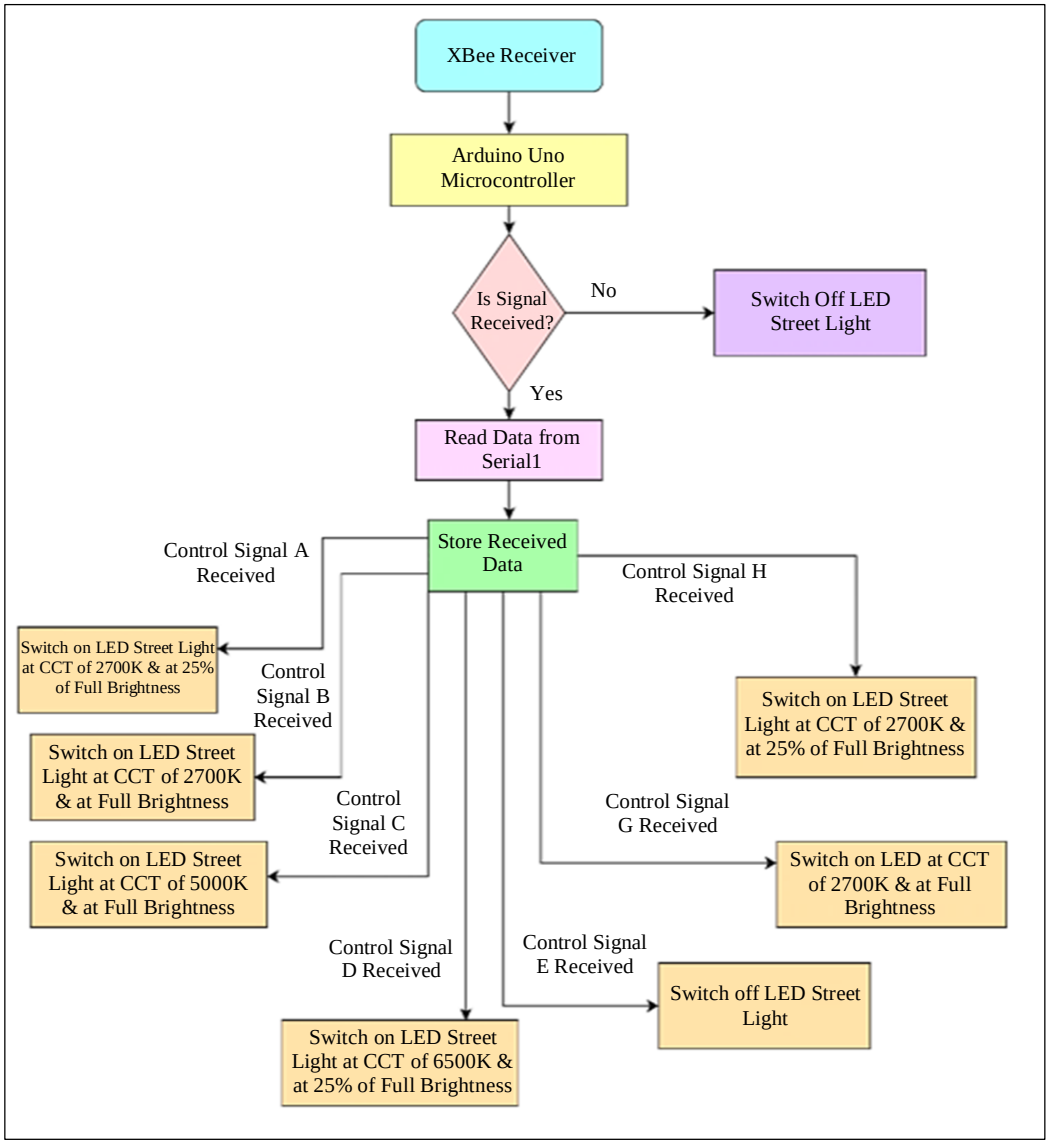

Fig. 4 Flowchart of XBee end device side microcontroller operation

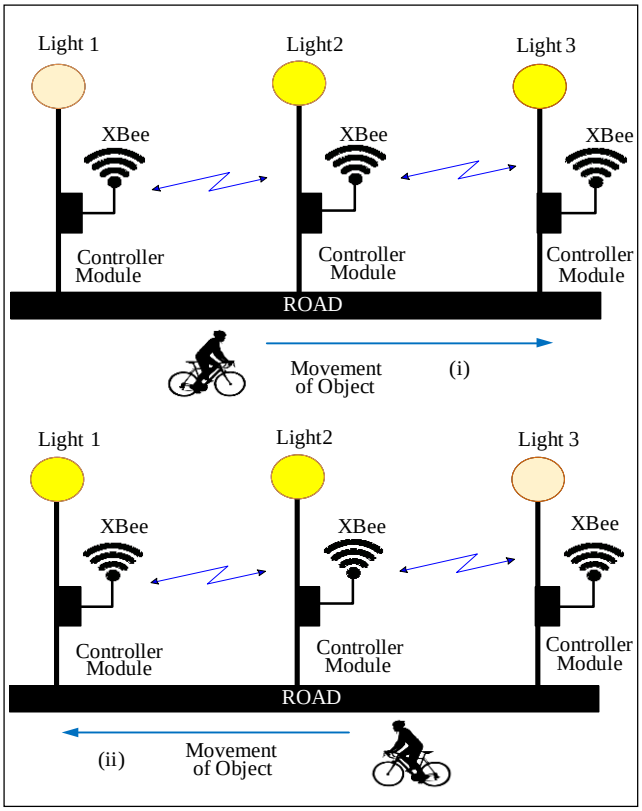

Fig. 5 Functioning of designed lighting system

In this designed system, all XBee modules connected to streetlighting poles can detect objects and adjust the brightness of the LEDs connected to them. They also send the same signals to the main microcontroller to indicate the presence of an object. The main microcontroller makes decisions about changing the status of other LEDs connected to the XBee network. This means that a two-way communication system is integrated into the developed system.

In this developed system, the ESP8266 initially collects data from the weather API to determine whether there is any fog present in the weather. The LED streetlights are controlled by the main microcontroller, which also receives all sensor data, including data from the ESP8266 IoT device. The ESP8266 is programmed to connect to a WiFi network to access the internet and make API requests specifically to collect fog data from the weather API's fog data endpoint. After verifying the API key, fog data is received from the weather API.

The main microcontroller receives fog information from the Node MCU and makes decisions about the presence of fog in the local area. If it senses fog is present, then switch on the LED at a CCT of 2700K to enhance visibility. Otherwise, it switches on LEDs with a CCT of 6500 K. In this control scheme, RGB color composition-based LEDs can vary red, green, and blue color to create different lighting effects, adjusting the color of light sources in response to visual demands [13].

In RGB LED streetlight studies, it is found that during foggy and rainy weather conditions, streetlights should illuminate at a lower CCT of 2700 K. This adjustment improves visibility, allowing street surface users to move and drive more easily compared to when the CCT is set at 6500 K [6, 7]. Street surface users can move and drive more easily than the CCT of 6500 K illuminated street surface. This design scheme can effectively enhance visibility when any adverse weather conditions arise.

5. Mathematical Modelling of Developed System

This developed system comprises an LDR sensor, a DHT11 sensor, a PIR sensor, and XBee wireless communication devices for transmitting signals generated to other streetlighting poles. Mathematical models for all input sensors are provided below:

5.1. LDR Sensor

LDR sensor senses the presence of light intensity and calculates resistance value depending on it.

Input: Light intensity (I)
Output: Resistance (R_{LDR})

Model:

$$R_{LDR} = R_0 \times \left(\frac{1}{I}\right)^{\alpha}$$

R_0 : Resistance of LDR in darkness
α : Sensitivity constant

5.2. DHT11 Sensor

DHT11 sensor senses local area temperature and humidity and sends it to the microcontroller. Temperature (T_{DHT}), Humidity (H_{DHT}) Model:

Temperature: $T_{DHT} = f_1(T_{\text{local env}}) + \epsilon_1$

Humidity: $H_{DHT} = f_2(H_{local\ env}) + \epsilon_2$

f_1 and f_2 : Functions representing sensor characteristics.
$T_{local\ env}$ and $H_{local\ env}$: Local environmental temperature and humidity.
ϵ_1 and ϵ_2: Errors at the time of measurement

5.3. PIR Sensor

LED brightness is controlled depending on the presence of an object at the detection zone of the PIR sensor. Let us denote:

$P_{PIR\ SENSOR}$: Output signal of the PIR sensor (1 for motion detected, 0 for no motion).

v: Speed or motion (meters per second) of detected object.

Let us consider $f(P_{PIR\ SENSOR}, v)$ is a function that represents the combinational effect of object presence and its speed on the sensor's output. This function could be a piecewise function to capture different object presence scenarios:

5.3.1. No Motion Detected

$$f(P_{PIR\ SENSOR}, v) = 0 \text{ if } P_{PIR\ SENSOR} = 0$$

If no motion is detected, the sensor shows that the output is zero.

5.3.2. Motion Detected

$$f(P_{PIR\ SENSOR}, v) = h(v) \text{ if } P_{PIR\ SENSOR} = 1$$

If the motion is detected, then consider the output as a function of h(v) that represents the sensor's response to different motions of the detected object.

Speed Sensitivity Function $(h(v))$

The function h(v) represents the sensitivity sensed by the PIR sensor at object speed. It could be denoted based on experimental data or theoretical assumptions. A few possible forms are outlined below:

Linear Function

$$h(v) = k \times v$$

k : Proportionality constant determining the sensitivity of the sensor at its speed.

This model assumes a linear relationship between object speed and sensor output.

Exponential Decay Function

$$h(v) = A \times e^{-\lambda v}$$

A: Amplitude of the signal.

λ : Decay constant determining how quickly the signal decreases with increasing speed.

This model assumes that the sensor's sensitivity decreases exponentially with speed. The function $h(v)$ depends on the characteristics of the PIR sensor and the specific needs of the application. Experimental data is required to determine the parameters of the speed sensitivity function.

Real-world factors such as the noise of the sensor and local environmental conditions may affect the sensor's response, and it should be considered in the modelling if it actually exists.

5.4. XBee Network Modelling

To create mathematical modelling of XBee wireless network, various factors need to be considered like signal propagation, interference and other characteristics of XBee modules. Details of mathematical modelling are provided below:

5.4.1. Modelling of Path Loss:

The received signal strength (P_{REX}) at the receiving side or receiver can be calculated using a path loss model using the Friis transmission equation:

$$P_{REX} = P_{TEX} - L + G + \epsilon_{REX}$$

P_{TEX}: Transmitted power.

L : Path loss.

G: Antenna gain.

ϵ_{REX}: Random noise at the receiver.

5.4.2. Path Loss (L)

The path loss (L) can be calculated using models like the free space path loss model or long-distance path loss model:

$$L = L_0 + 10m \log_{10}\left(\frac{d}{d_0}\right)$$

L_0 : Reference path loss at the reference distance d_0.

m : Exponent of Path loss.

d : Distance between transmitter and receiver.

5.4.3. Wireless Communication

The XBee modules use wireless protocols like Zigbee for communication purposes. The success rate of packet transmission (P_{success}) can be modelled considering factors like Signal-to-Noise Ratio (SNR) and interference: $P_{\text{success}} = f(SNR, \text{interference})$.

5.4.4. Interference

Interference (I) can be modelled using the sum of the interfering signals from other sources:

$$I = I_1 + I_2 + \cdots + I_n$$

5.4.5. Signal-to-Noise Ratio (SNR)

SNR is the ratio of received signal power to noise power:

$$SNR = \frac{P_{REX}}{\sigma^2}$$

σ^2 : Noise power.

5.4.6. Transmitted Power (P_{TX})

The transmitted power depends on the configuration of the XBee module and is a constant value.

5.4.7. Antenna Gain (G)

The antenna gain represents the directionality of the antenna and affects the signal strength.

5.4.8. Random Noise (ϵ_{RX})

Random noise at the receiver is modelled as Gaussian noise with zero mean and variance σ^2.

5.4.9. Type of Network Topology

Considerations such as the number of nodes, their actual locations, and the type of network topology (mesh, star, etc.) influence the signal propagation and the network performance.

5.4.10. Packet Loss Rate

Based on the success rate of packet transmission, we can calculate the packet loss rate (P_{loss}).

Considerations

- Environmental factors such as the presence of obstacles and multipath propagation affect signal propagation.
- Parameters like path loss exponent, antenna characteristics, and interference levels need calibration based on empirical data.
- Adjustment needs to be considered in the case of real-world scenarios as the model normally assumes ideal conditions.

6. Developed Prototype Model

Based on control logic, two sets of prototype models have been designed and shown in Figures 6 and 7 below.

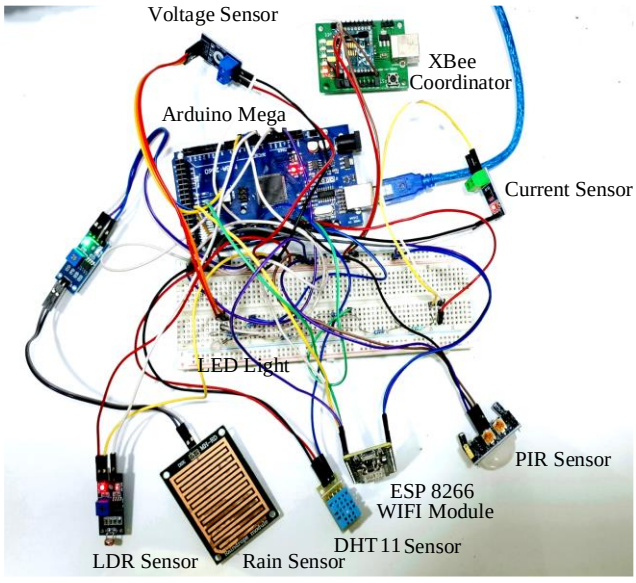

Fig. 6 XBee coordinator side microcontroller connected with different sensors

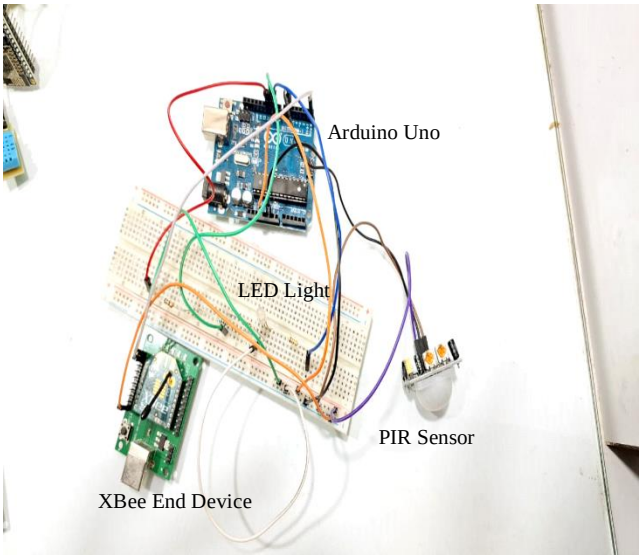

Fig. 7 XBee end device side microcontroller

The prototype models depicted in Figures 6 and 7 are intended for the XBee coordinator-side main microcontroller and the XBee end device-side microcontroller, respectively.

These models were designed and experimentally tested to ensure proper functioning. During testing, both models responded satisfactorily, and the test results are depicted in the figures below through a graphical presentation.

7. Performance Analysis of the Designed Prototype Model

For the performance analysis of the developed system, several experiment setups were arranged and conducted to collect real-time data from all sensor modules and the connected LEDs of the prototype model.

1. Data from all connected sensors were measured and recorded over a certain period at different operating conditions.
2. The current, voltage, and power consumed by the LED connected to the main microcontroller were also measured and recorded over a certain period for electrical parameter analysis purposes at different operating conditions.
3. The response of both the XBee coordinator side and end-device side was recorded over a certain period for analysis.

PIR sensor data was collected from the experimental setup over a certain period. The recorded data is then plotted and shown in Figure 8.

Data sensed by the LDR sensor and rain sensor during rainy times are collected and plotted in Figure 9.

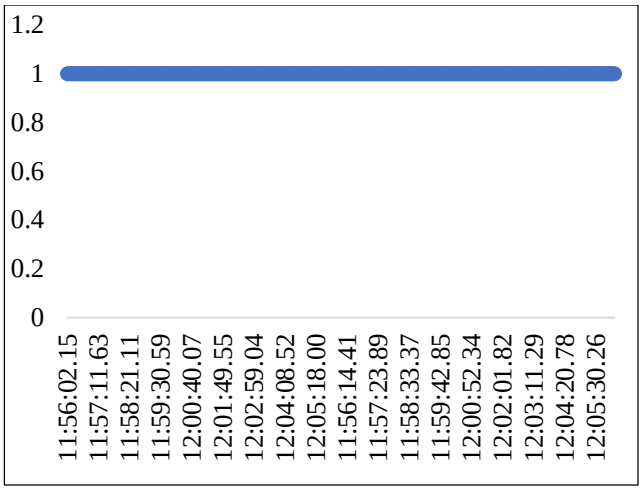

Fig. 8 Graphical analysis of PIR object detection sensor data

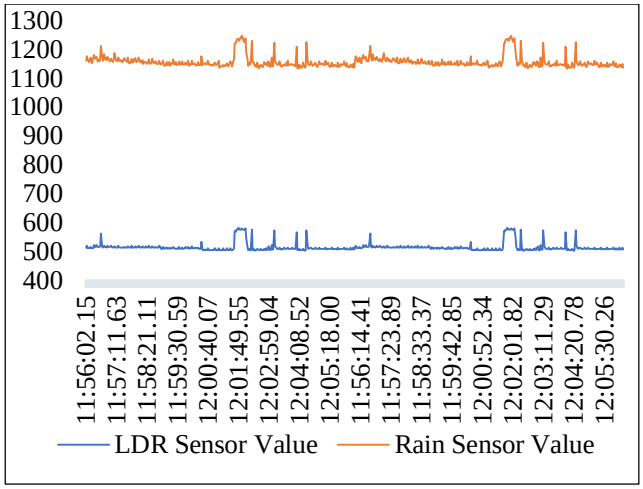

Fig. 9 Graphical analysis of LDR sensor and rain sensor data

The data readings from the DHT11 sensor are recorded and plotted in Figures 10 and 11.

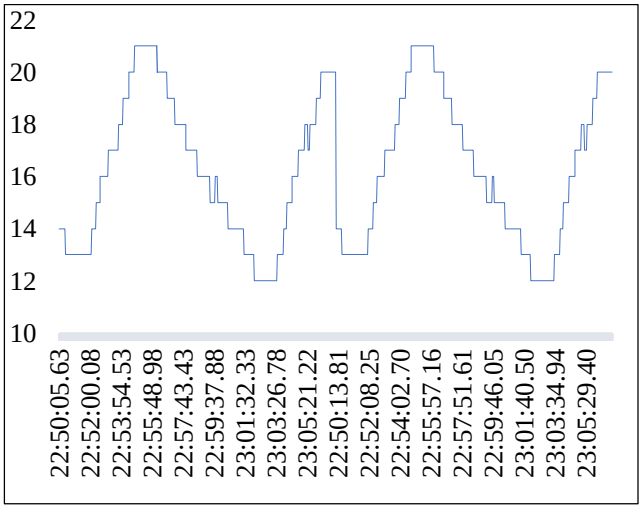

Fig. 10 Graphical analysis of humidity data of DHT11 sensor

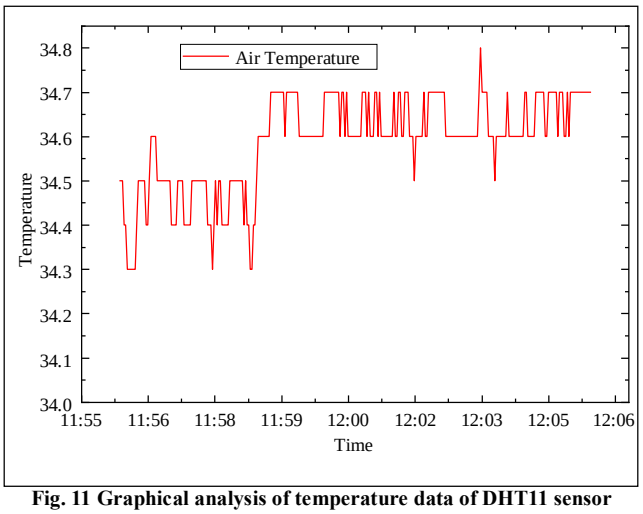

Fig. 11 Graphical analysis of temperature data of DHT11 sensor

The switching time of LEDs at both the main microcontroller side and the XBee end-device side was recorded and plotted in Figure 12.

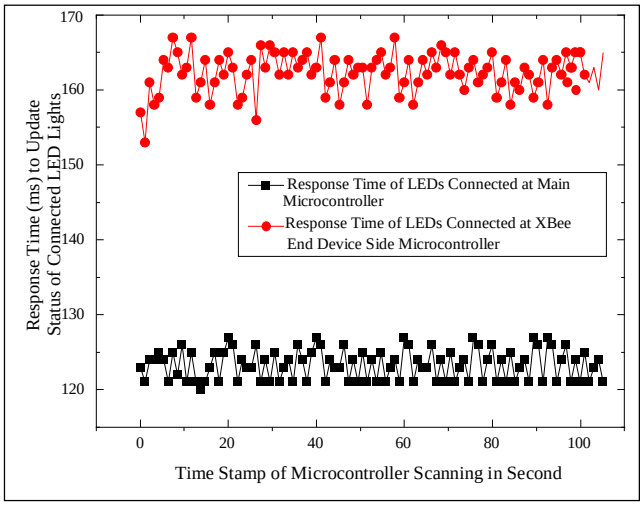

Fig. 12 Graphical analysis response time of LEDs connected at main microcontroller and XBee end device side microcontroller

The above graphical analysis indicates that all sensors and XBee modules are functioning satisfactorily, and they are successfully sending and receiving data. Based on the control logic setup of the developed system, the LED lights operate in three modes: switched off during daytime, dimmed to 25% of full brightness when no object is present, and at full brightness when objects are detected in low light conditions or at nighttime. In each condition, the LED will consume a different amount of current, have a different voltage across it, and consume a different amount of power. All electrical parameters have been recorded and are shown below in a graphical representation. The current and power consumed and voltage across the green channel of RGB LED during daytime are recorded and shown in Figures 13, 14 and 15 respectively.

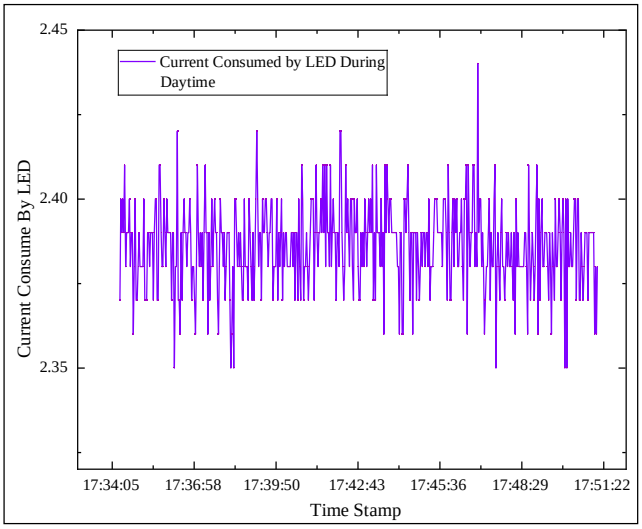

Fig. 13. Graphical analysis of current consumed by led during daytime

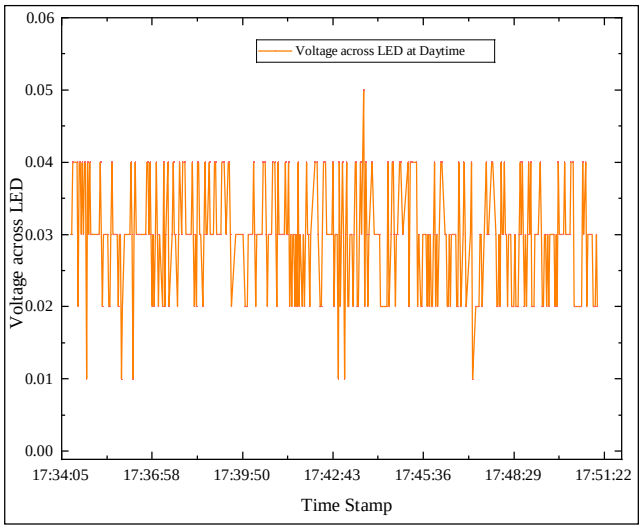

Fig. 14. Graphical analysis of voltage across LED during daytime

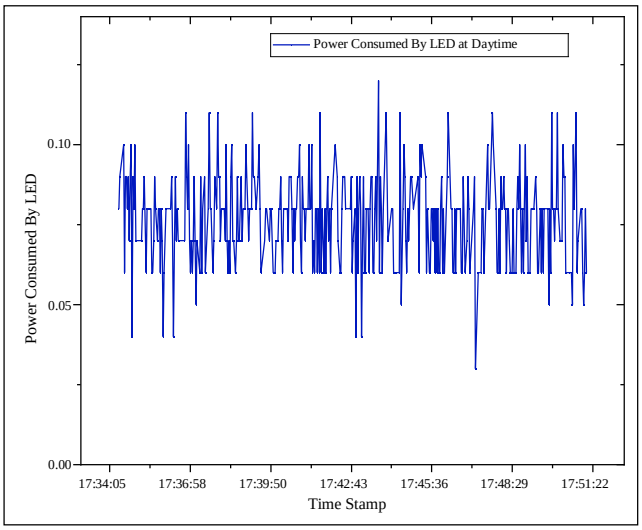

Fig. 15 Graphical analysis of power consumed by LED during daytime

The total power consumed by LED at the daytime is very less, as shown in the above graphical analysis. The current, power consumed, and voltage across the green channel of RGB LED when dimmed to 25% of full brightness and with a CCT of 6500K are recorded and shown as graphical presentations in Figures 16,17 and 18, respectively.

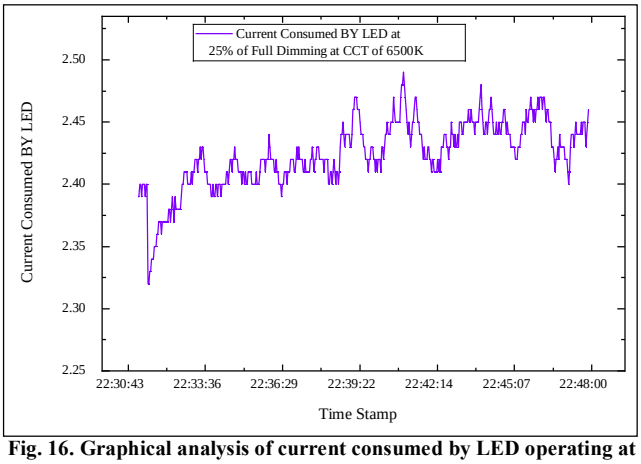

Fig. 16. Graphical analysis of current consumed by LED operating at 25% of full dimming & at CCT of 6500K

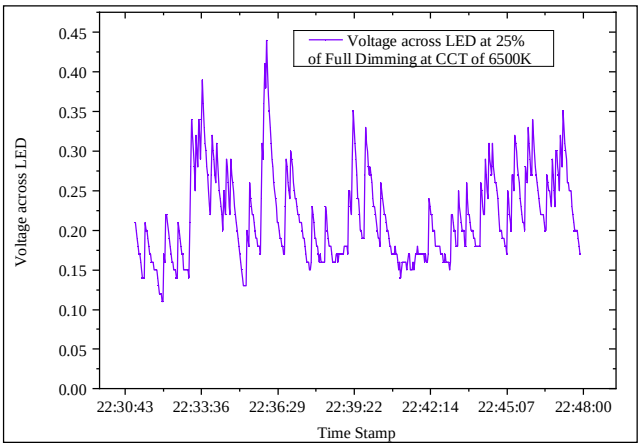

Fig. 17 Graphical analysis of voltage across LED at 25% dimming of full brightness with a CCT of 6500K

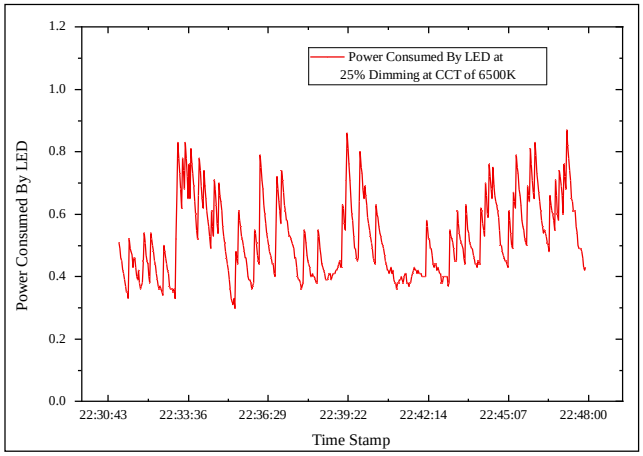

Fig. 18 Graphical analysis of power consumed by LED operating at 25% of full dimming and at CCT of 6500K

The total power consumed by the LED when dimmed to 25% of its full brightness exceeds the power consumed during the day, as depicted in the graphical analysis above. The current and power consumed and voltage across green channel LED when operating at full brightness are recorded and shown as graphs in Figures 19, 20 and 21 , respectively.

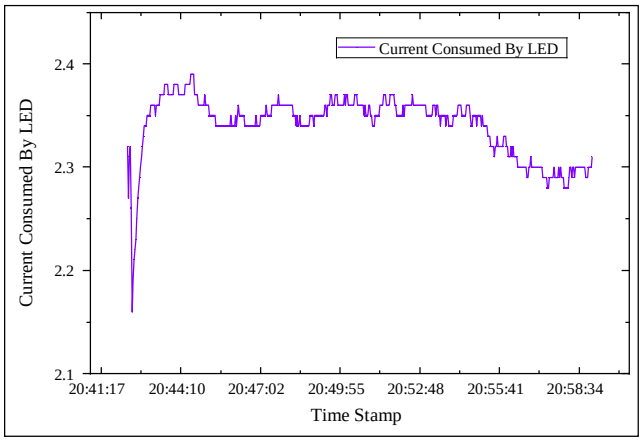

Fig. 19 Graphical analysis of current consumed by LED at full brightness & CCT of 6500K

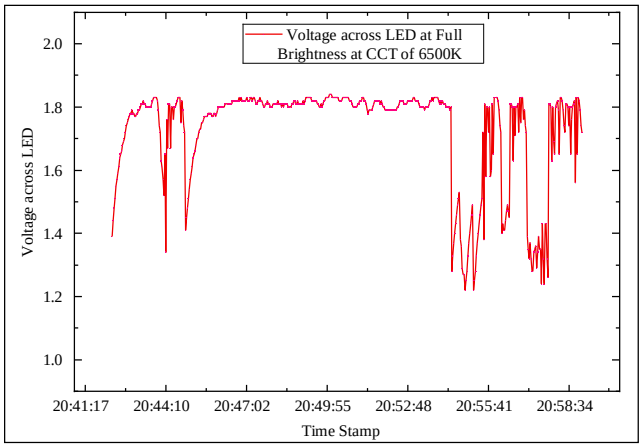

Fig. 20 Graphical analysis of voltage across LED at full brightness with a CCT of 6500K

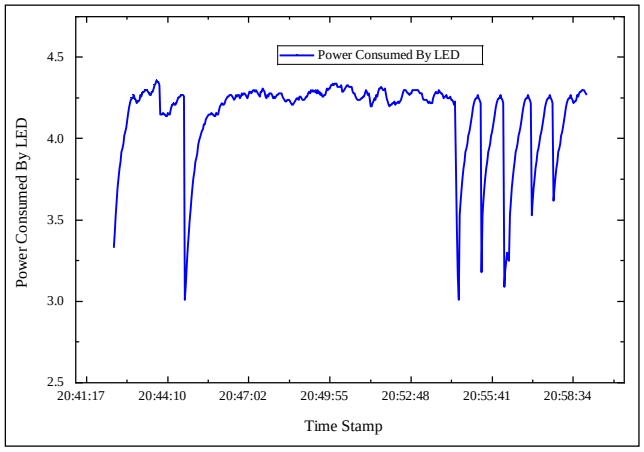

Fig. 21 Graphical analysis of power consumed by LED at full brightness & CCT of 6500K

During a rainy period when the sky was very dark, adverse weather data were collected under very low light conditions. The data of current power consumed, and data of voltage across the green channel LED were recorded when dimmed to 25% of full brightness and with a CCT of 2700K. The recorded data are plotted as shown in Figures 22, 23 and 24, respectively.

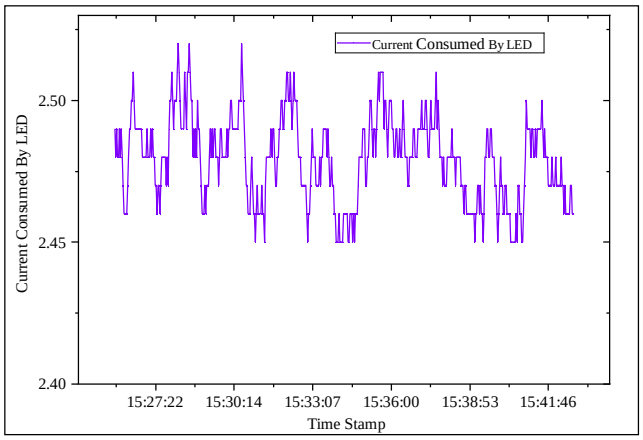

Fig. 22 Graphical analysis of the current consumed by the LED at 25% dimming of full brightness and at a CCT of 2700K

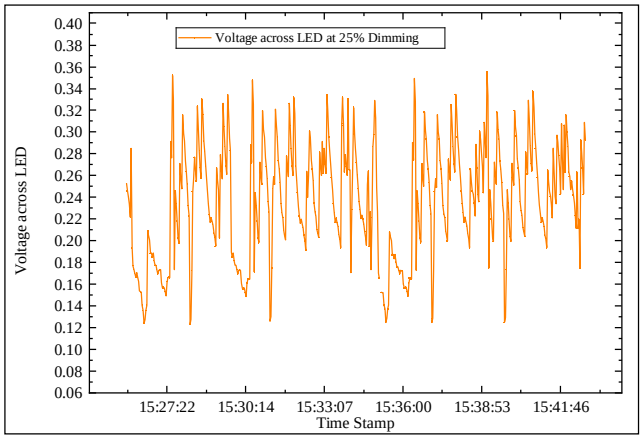

Fig. 23 Graphical analysis of the voltage across LED at 25% dimming of full brightness and at a CCT of 2700K

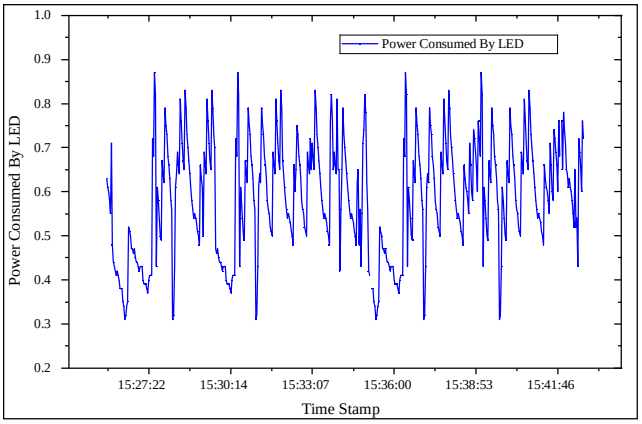

Fig. 24. Graphical analysis of the power consumed by the LED at 25% dimming of full brightness and at a CCT of 2700K

The current and power consumed and the voltage across the green channel LED when operating at full brightness and at CCT of 2700K are recorded and plotted in Figures 25, 26 and 27, respectively.

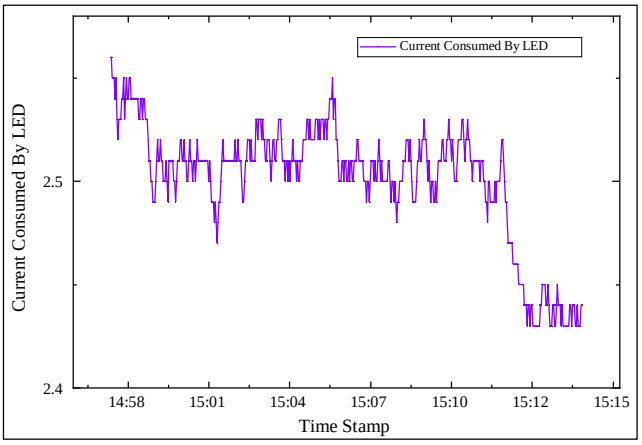

Fig. 25 Graphical analysis of current consumed by LED at full brightness & at CCT of 2700K

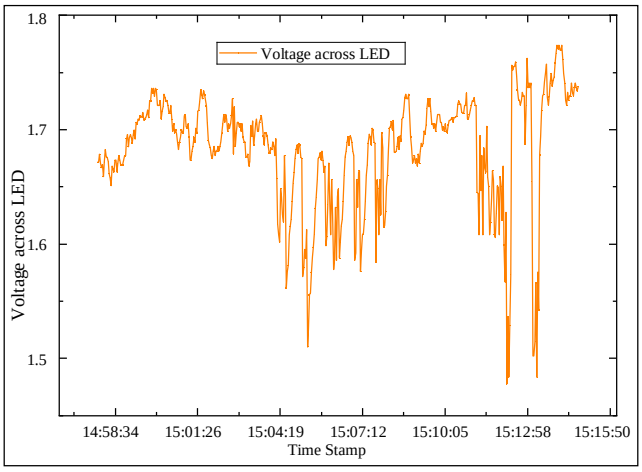

Fig. 26 Graphical analysis of voltage across LED at full brightness with a CCT of 2700K

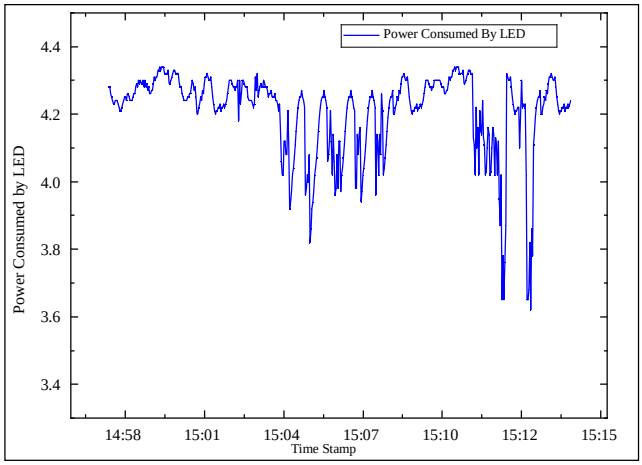

Fig. 27 Graphical analysis of power consumed by LED at full brightness with a CCT of 2700K

During the experimental process, the current consumed and voltage across each color channel of the RGB LED were recorded for both CCTs of 6500K and 2700K. In both color adjustment settings, the power consumed by each channel of the RGB LED was also recorded. For a specific brightness and color adjustment condition to plot the graph of current, voltage, and power, 500 numbers of data points were collected, which is too many to include in this paper. Some data measured with a multimeter are shown in Table 1.

All the graphical analyses of current, voltage, and power shown in the figures above from Figures 13 to 27 are based on data from current and voltage sensors connected across each channel of the RGB LED and recorded over a certain period. The current power consumed and the voltages across the green channel of the LED are plotted in these figures.

The graphical analysis is depicted in Figures 18 and 21, where the LED is dimmed to 25% of full brightness, and in Figures 24 and 27, where the LED is operating at full brightness condition. The data readings recorded by the multimeter are shown in Table 1. This reading suggests that when the brightness of the LED is increased, the power consumed by the LED is also increased, and when the color of the LED is shifted from cool white to warm white, then there is a slide reduction of the power consumption of the LED with the shift in Correlated Color Temperature (CCT) from 6500K to 2700K. This means the designed system will not consume extra power from the supply while also improving visibility for street surface users during adverse weather conditions.

Additionally, when the developed system dims the LED lights at night time when no objects or human beings are present on the street surface, it consumes less power compared to a timer-based street lighting system. This type of adjustment makes the design energy-efficient. After analyzing the graphical representations in Figures 15, 18, Figures 21, 24 and 27, it becomes evident that the power consumed by the LED is directly proportional to the brightness of the LED. Merely increasing the brightness of the LED light source in foggy and rainy weather is insufficient [27].

In this work, the CCT (Correlated Color Temperature) of the LED light is changed from cool white to warm white without altering the electrical energy consumption. This adjustment improves visibility in adverse weather conditions, making the system more energy-efficient compared to a normal lighting system, where all street lights are switched on throughout the night and consume a significant amount of power, leading to higher electricity costs.

The designed system will light up at full brightness only when it senses movement on the street. If no object is present on the street, the lighting system will adjust the brightness to 25% to save energy. At night, this adjustment can reduce electricity consumption depending on the duration of both

object detection time and no object detection time. A comparison of the electrical energy consumed by both the normal lighting system and the designed lighting system is depicted in Figure 28.

Table 1. Electrical parameters of RGB LED under different operating conditions

Sr. No.	LED Brightness Level (%)	Operating at CCT of 6500K				Operating at CCT of 2700K			
		Power Consumed by Red channel Pin (mW)	Power Consumed by Green Channel Pin (mW)	Power Consumed by Blue Channel Pin (mW)	Total Power Consumed by LED (mW)	Power Consumed by Red channel Pin (mW)	Power Consumed by Green channel Pin (mW)	Power Consumed by Blue channel Pin (mW)	Total Power Consumed by LED (mW)
1	0	0.09	0.1	0.08	0.27	0.1	0.08	0.08	0.26
2	25	0.76	0.71	0.74	2.21	0.78	0.69	0.62	2.09
3	100	4.43	4.36	4.21	13	4.24	3.96	3.84	12.04

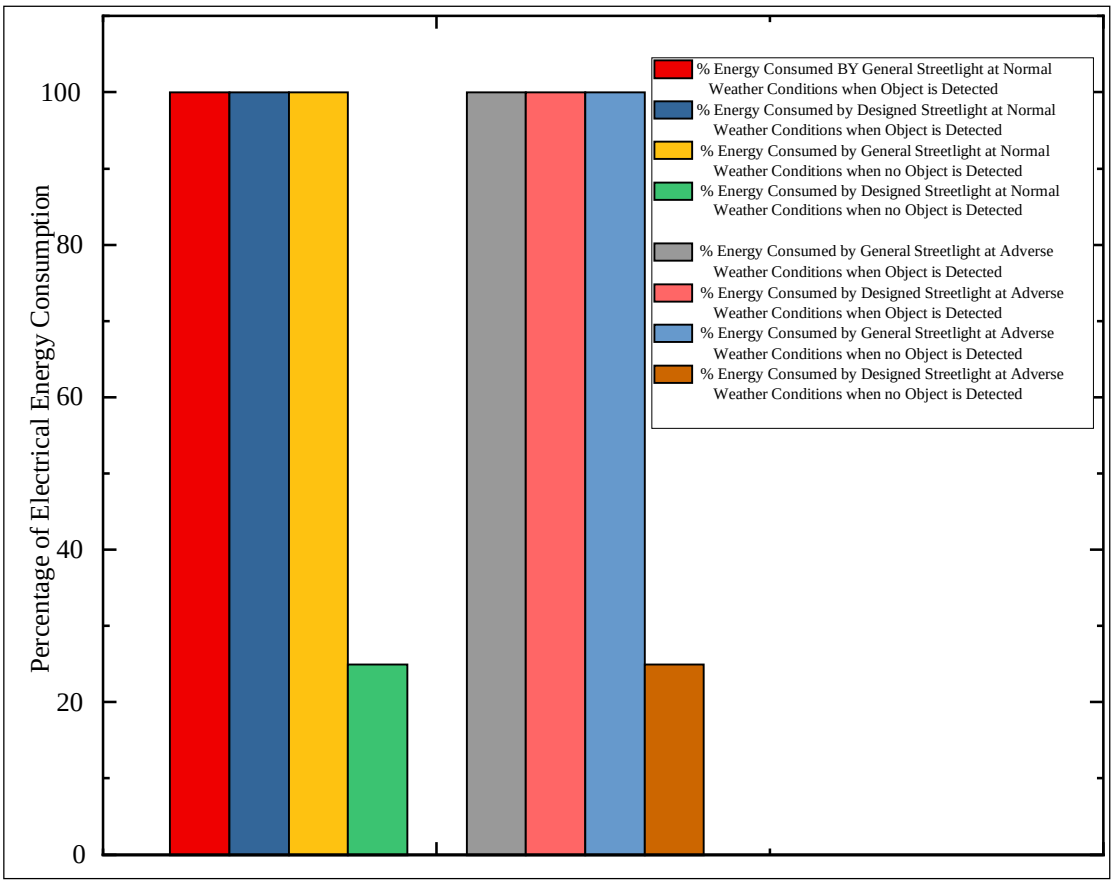

Fig. 28 Comparison of electrical energy consumed by normal lighting system and designed lighting system in different weather conditions

8. Conclusion

This work introduces an intelligent street lighting solution with variable color temperature to enhance visibility in adverse weather conditions, all while keeping electrical energy consumption in check. A functional hardware prototype model has been developed, operating based on developed control logic and real-time street surface conditions. The LED lighting is intelligently adjusted in response to the presence of objects, dimming when necessary. Moreover, brightening as needed. This dynamic control setup will significantly improve visibility over the street surface, thereby conserving energy. Additionally, it will be capable of reducing traffic accidents that commonly occur during foggy and rainy weather. By dynamically adapting to environmental conditions and traffic presence, this smart lighting system will not only enhance visibility but also contribute to maintaining traffic speed.

Overall, this intelligent street lighting solution offers a comprehensive approach to addressing visibility challenges during adverse weather conditions, demonstrating its potential to enhance street safety while conserving energy.

References

[1] Zeeshan Kaleem, Tae Min Yoon, and Chankil Lee, "Energy Efficient Outdoor Light Monitoring and Control Architecture Using Embedded System," *IEEE Embedded Systems Letters*, vol. 8, no. 1, pp. 18-21, 2016. [CrossRef] [Google Scholar] [Publisher Link]

[2] Fabio Leccese, "Remote-Control System of High Efficiency and Intelligent Street Lighting Using a ZigBee Network of Devices and Sensors," *IEEE Transactions on Power Delivery*, vol. 28, no. 1, pp. 21-28, 2013. [CrossRef] [Google Scholar] [Publisher Link]

[3] Rune Elvik, "Meta-Analysis of Evaluations of Public Lighting as Accident Countermeasure," *Transportation Research Record*, no. 1485, pp. 112-123, 1195. [Google Scholar] [Publisher Link]

[4] Paul C. Box, "Major Accident Reduction by Illumination," *Transportation Research Record*, no. 1247, pp. 32-38, 1989. [Google Scholar] [Publisher Link]

[5] Paul C. Box, "Freeway Accidents and Illumination," *Highway Research Record*, no. 416, pp. 10-20, 1972. [Google Scholar][Publisher Link]

[6] Wonil Park et al., "Investigating the Effect of Road Lighting Color Temperature On-Road Visibility in Night Foggy Conditions," *Applied Ergonomics*, vol. 106, 2023. [CrossRef] [Google Scholar] [Publisher Link]

[7] Johan Casselgren et al., "Road Condition Analysis Using NIR Illumination and Compensating for Surrounding Light," *Optics and Lasers in Engineering*, vol. 77, pp. 175-182, 2016. [CrossRef] [Google Scholar] [Publisher Link]

[8] Subramanian Muthu, Frank J.P. Schuurmans, and Michael D. Pashley, "Red, Green, and Blue LEDs for White Light Illumination," *IEEE Journal on Selected Topics in Quantum Electronics*, vol. 8, no. 2, pp. 333-338, 2002. [CrossRef] [Google Scholar] [Publisher Link]

[9] Biao Sun et al., "Investigation on Fog Formation of LNG Ambient Air Vaporisers," *Applied Thermal Engineering*, vol. 193, 2021. [CrossRef] [Google Scholar] [Publisher Link]

[10] M. Segal, E. Ganor, R.J. Pohoryles, "Evaluation of a Numerical Fog Forecast Model and Its Application to Operational Fog Prediction," *Journal of Applied Meteorology and Climatology*, vol. 45, no. 10, pp. 1365-1381, 2006.

[11] A.H. Perry, L.J. Symons, *Highway Meteorology*, 1st ed., Routledge - Taylor & Francis Group, 1991. [Google Scholar] [Publisher Link]

[12] S.S. Chand, R.H.Y. So, "Automatic Outdoor Lighting Control System Using DHT11 Sensor," *2011 International Conference on Mechatronics and Automation*, pp. 2353-2357, 2011.

[13] Xiaohui Qu, Siu Chung Wong, and Chi K. Tse, "Color Control System for RGB LED Light Sources Using Junction Temperature Measurement," *IECON 2007 - 33rd Annual Conference of the IEEE Industrial Electronics Society*, Taipei, Taiwan, pp. 1363-1368, 2007. [CrossRef] [Google Scholar] [Publisher Link]

[14] T. Adams et al., "*Lighting of Roads for Motor and Pedestrian Traffic*," 2nd ed., Technical Report, CIE, 2010. [Publisher Link]

[15] Robert Faludi, *Building Wireless Sensor Networks: A Practical Guide to the Zigbee Mesh Networking Protocol*. Published O'Reilly Media, Inc., 2011. [Google Scholar] [Publisher Link]

[16] Yu-Sheng Yang et al., "An Implementation of High Efficient Smart Street Light Management System for Smart City," *IEEE Access*, vol. 8, pp. 38568-38585, 2020. [CrossRef] [Google Scholar] [Publisher Link]

[17] Md Arafatur Rahman et al., "IoT-Enabled Light Intensity-Controlled Seamless Highway Lighting System," *IEEE Systems Journal*, vol. 15, no. 1, pp. 46-55, 2021. [CrossRef] [Google Scholar] [Publisher Link]

[18] Wout van Bommel, *Road Lighting' Fundamentals, Technology and Application*, 1st ed., Springer Cham, 2015. [CrossRef] [Google Scholar] [Publisher Link]

[19] International Commission on Illumination, "*A Unified Framework of Methods for Evaluating Visual Performance Aspects of Lighting*," Technical Report, 1972.

[20] J.R. Coaton, M.A. Cayless, and A.M. Marsden, *Lamps and Lighting*, Routledge - Taylor & Francis Group, 2012. [Google Scholar] [Publisher Link]

[21] Yuxi Jiang et al., "An Energy-efficient Street Lighting Approach Based on Traffic Parameters Measured by Wireless Sensing Technology," *IEEE Sensors Journal*, vol. 21, no. 17, pp. 19134-19143, 2021. [CrossRef] [Google Scholar] [Publisher Link]

[22] Luiz Fernando Pinto de Oliveira, Leandro Tiago Manera, and Paulo Denis Garcez Da Luz, "Development of a Smart Traffic Light Control System with Real-Time Monitoring," *IEEE Internet of Things Journal*, vol. 8, no. 5, pp. 3384-3393, 2021. [CrossRef] [Google Scholar] [Publisher Link]

[23] Suntiti Yoomak, and Atthapol Ngaopitakkul, "Optimization of Lighting Quality and Energy Efficiency of LED Luminaires in Roadway Lighting Systems on Different Road Surfaces," *Sustainable Cities and Society*, vol. 38, pp. 333-347, 2018. [CrossRef] [Google Scholar] [Publisher Link]

[24] Hiroki Noguchi, and Toshihiko Sakaguchi, "Effect of Illuminance and Color Temperature on Lowering of Physiological Activity," *Applied Human Science*, vol. 18, no. 4, pp. 117-123, 1999. [CrossRef] [Google Scholar] [Publisher Link]

[25] Huaizhou Jin et al., "Research on the Lighting Performance of LED Street Lights With Different Color Temperatures," *IEEE Photonics Journal*, vol. 7, no. 6, pp. 1-9, 2015. [CrossRef] [Google Scholar] [Publisher Link]

[26] IEEE, "*IEEE Standard for a Smart Transducer Interface for Sensors and Actuators Wireless Communication Protocols and Transducer Electronic Data Sheet (TEDS) Formats*," IEEE Std 1451.5-2007, pp. 1-225, 2007. [CrossRef] [Publisher Link]

[27] Dipanjan Saha, Sk Mahammad Sorif, and Pallav Dutta, "Weather Adaptive Intelligent Street Lighting System with Automatic Fault Management Using Boltuino Platform," *2021 International Conference on ICT for Smart Society (ICISS)*, Bandung, Indonesia, pp. 1-6, 2021. [CrossRef] [Google Scholar] [Publisher Link]